



Low-energy ammonium recovery by a combined bio-electrochemical and electrochemical system

S. Georg^{a,b}, A.T. Puari^a, M.P.G. Hanantyo^a, T. Sleutels^a, P. Kuntke^{a,b,*}, A. ter Heijne^b, C.J.N. Buisman^{a,b}

^a Wetsus, European Centre of Excellence for Sustainable Water Technology, P.O. Box 1113, 8900 CC Leeuwarden, The Netherlands

^b Environmental Technology, Wageningen University, P.O. Box 17, 6700 AA Wageningen, The Netherlands

ARTICLE INFO

Keywords:

Bio-electrochemical systems
Ammonium recovery
Sequential treatment
Electrodialysis
Integration of bio-electrochemical and electrochemical system

ABSTRACT

Bio-electrochemical systems (BESs) can recover ammonium at low specific energy inputs and can produce hydrogen gas. A reason hampering development of large-scale applications for ammonium recovery is the general instability of the bio-generated current and the thereby variable TAN (ammonia and ammonium) effluent concentrations. Electrochemical systems for ammonium recovery, such as the hydrogen recycling electrochemical system (HRES), can fine-tune the applied current, but require higher specific energy inputs than BES, and may require an additional external hydrogen supply in case of HRES. This research presents for the first time an integrated BES and HRES system for ammonium recovery to combine the advantages of both types of systems to achieve high TAN removal efficiency at low specific energy input. The HRES was able to partially compensate for BES instability, which resulted in an overall high TAN removal efficiency (89–95 %) at an increased energy demand of 5.2–10.2 MJ/kg_N. When the BES was performing stably and efficiently, the HRES removed almost all of remaining TAN at up to 99.8 % overall TAN removal efficiency, requiring 9.2 MJ/kg_N. The combined system can remove TAN down to much lower effluent concentrations at little to no additional energy input. These results indicate that combining BES and HRES in one system can result in TAN recovery that is more efficient than in each system separately, which could facilitate new application possibilities for (bio-)electrochemical ammonium recovery.

1. Introduction

The growing human population is breaching the planetary boundary for use of reactive nitrogen (N_r, for example ammonia, nitrite or nitrate, [39]). This breach causes eutrophication, loss of biodiversity, and is partially responsible for anthropogenic climate change [30] with the main cause being anthropogenic fertilizer application in agriculture [2]. Current fertilizer production is carried out in a linear nitrogen (N) economy [38] of atmospheric gaseous N₂ activation to ammonia (NH₃), mostly through the Haber–Bosch (HB) process, and application of NH₃ as fertilizer. However, only a fraction of the NH₃ in fertilizer is converted into agricultural products and the N_r ultimately deteriorating the environment. Therefore, stringent discharge limits are imposed on N_r, leading to wastewater treatment and N₂ production. This linear process of N activation and de-activation is energy-intensive with 27 MJ/kg_N for HB (best available technology [9]) and 45 MJ/kg_N for nitrification–denitrification [22] or 16 MJ/kg_N for Sharon/anammox [22],

respectively. HB alone requires around 2 % of the annual global energy consumption [3] and both HB and NH₃ de-activation contribute to climate change via greenhouse gas emissions [9,40]. This linear economy can be partly transformed by recovering NH₃ directly from its source in a circular N economy approach as directly applicable, valuable fertilizer.

A promising technology to separate NH₃ from wastewater for recovery is electrodialysis (ED), where an applied electrical current drives NH₄⁺ ions as part of total ammonia nitrogen (TAN, as sum of NH₄⁺ and NH₃) across a cation exchange membrane (CEM) and thereafter can be recovered. One recovery method that has been demonstrated combined with ED is liquid/liquid membrane contactor (LLMC). The LLMC principle is based on NH₃ diffusion across a hydrophobic membrane and results in an acidic ammonium solution [27,29]. The energy consumption of TAN recovery with ED and LLMC (13–24 MJ/kg_N [4,7,17,21]) is lower than for TAN removal and inactivation by nitrification–denitrification and re-activation by HB. ED is scalable because the

* Corresponding author.

E-mail address: Philipp.kuntke@wur.nl (P. Kuntke).

<https://doi.org/10.1016/j.cej.2022.140196>

Received 22 August 2022; Received in revised form 28 October 2022; Accepted 31 October 2022

Available online 15 November 2022

1385-8947/© 2022 The Author(s). Published by Elsevier B.V. This is an open access article under the CC BY license (<http://creativecommons.org/licenses/by/4.0/>).

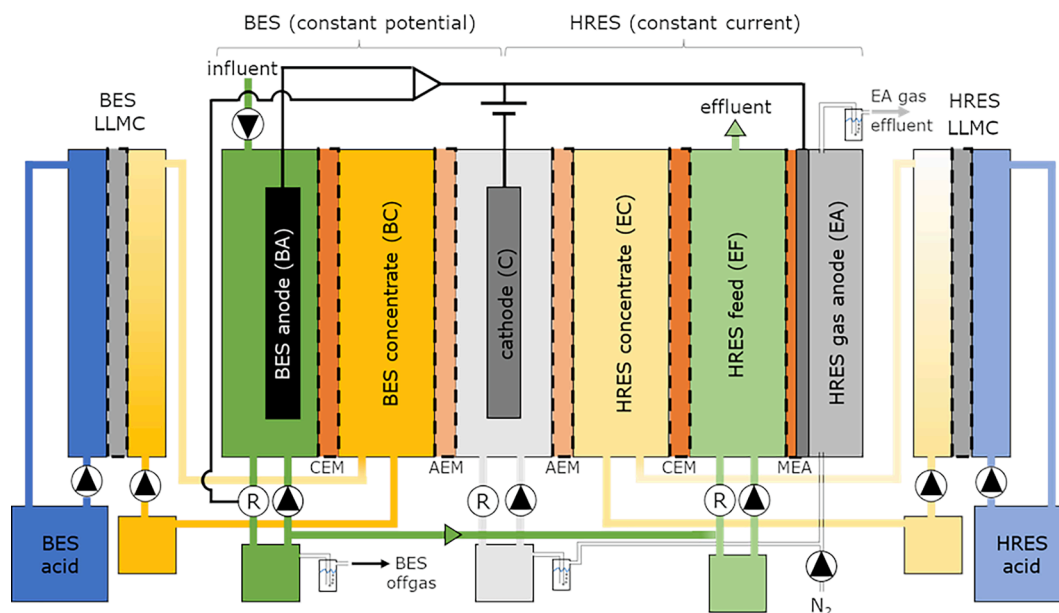


Fig. 1. Schematic depiction of experimental setup. Medium was fed into the bio-electrochemical system (BES) anode compartment and its effluent then fed into the hydrogen recycling electrochemical system (HRES) feed. The potentiostatically controlled bio-anode and the galvanostatically controlled electrochemical membrane electrode assembly (MEA) both shared the same counter electrode as cathode. Currents generated in the bio-anode and MEA HRES-feed caused migration of ions across their respective cation exchange membranes (CEMs) into their respective concentrate compartments towards the cathode. The cathode compartment was located between two anion exchange membranes (AEMs) towards each concentrate. Each concentrate was recirculated through liquid/liquid membrane contactors (LLMC) units for TAN recovery. The AEMs promoted hydroxyl anion transport to the concentrates, increasing their pH for improved TAN recovery, and permitted separate recirculation of cathodically generated hydrogen gas to the MEA.

driving force for this process, the current, can be controlled and can therefore be adjusted to different loading conditions [31]. The current is usually generated by the water splitting reaction, oxygen evolution reaction at the anode and hydrogen evolution reaction at the cathode. However, the typically applied anode potentials necessary for water splitting can oxidize halogens, such as chloride and create toxic chlorine gas, chlorinated compounds, as well as adsorbable organohalogenes [1,43]. An improvement of ammonium recovery with ED in terms of required energy input and avoided electrochemical side reactions is the hydrogen recycling electrochemical system (HRES). In HRES, the overall theoretical required voltage input is 0 V since anode and cathode reaction have the same standard potential. Thereby, energy losses depend solely on the electrode overpotentials, transport potential, ionic resistance and pH gradient overpotentials generated, as well as the H_2 lost during cycling of H_2 between cathode and anode. Furthermore, electrochemical side reactions with halogens are avoided [15,16]. Therefore, this system can further save on energy input (9.7 MJ/kg_N, [33]) and the recovered TAN can close the cycle between wastewater TAN removal and TAN supply for fertilizer use. However, HRES only removes ions and an external H_2 supply is required.

Even lower energy inputs are achievable with bio-electrochemical systems (BESs) for ammonium recovery (down to 4 MJ/kg_N [42,44]) since the anodic reaction is the oxidation of bio-degradable organic matter (expressed as chemical oxygen demand (COD)) at low anode overpotentials [13]. Furthermore, from a wastewater treatment perspective, BESs can also remove COD from the wastewater, which further improves the effluent quality compared to ED and HRES. In addition, H_2 can be generated at the cathode if the BES is operated as microbial electrolysis cell (MEC, [20,36]), which can be viewed as energy output [28,37].

In BES, the current used to separate TAN is generated from organic substances by microorganisms. Ideally, all available substrate would be converted to current (with 100 % COD removal efficiency and 100 % Coulombic Efficiency), and each electron would drive one ammonium across the CEM (100 % transport efficiency). However, the current in

BES, which is the main rate determining factor, is highly dependent on the availability of biodegradable COD in the wastewater [10]. When the BES is operated at constant anode polarization, changes in COD availability lead to variable currents and consequently varying TAN removal rates and efficiencies [18,34,42]. These instabilities in generated current are, for example, caused by fluctuations in feed composition [15], pH [11], microbial community [26] or biofilm morphology [23,25].

The load ratio (L_N , ratio of electrical current and TAN loading) indicates how efficiently TAN can be removed from the respective wastewater [34]. Generating a current from wastewater COD in the BES and feeding an equal charge of TAN into the BES would mean applying a L_N of 1. Applying a L_N greater than 1 could, theoretically, remove all TAN fed into the system by driving it across a CEM. However, in practice, the necessary applied current to remove TAN can be lower due to TAN removal by diffusion, higher due to co-migration of non-TAN ions, or be limited at certain TAN removal efficiencies mostly independent from applied L_N s. Therefore, applying a L_N of 1.3 has been previously reported as optimum for highest TAN removal efficiency at lowest required energy input for the example of synthetic urine [35]. However, this optimum can change depending on variations in system configuration and operation, as well as wastewater composition [34,35]. Unlike in ED, the current in BES cannot be directly controlled, and therefore the resulting L_N and consequently TAN removal efficiencies will vary.

Combining ammonium recovery in BES with HRES can compensate for the other technology's disadvantage: BES in MEC mode can remove COD and TAN from a wastewater at low energy input and generate H_2 gas, but at fluctuating electrical currents. HRES can remove TAN at constant electrical current, but requires higher energy inputs compared to BES. The combination of both systems can thus lead to improved operation in terms of required energy input, TAN removal efficiency and effluent quality: TAN that is not removed in the BES could be removed in HRES and the additional H_2 gas supply for HRES could come from H_2 generated at the BES cathode. If BES and HRES shared the same cathode as counter electrode, the spatial footprint could be reduced, leading to

material and operational cost savings. This novel combined system has the potential to operate at high TAN removal efficiency and low TAN effluent concentrations at minimal energy input.

For this combination to make use of the benefits of both technologies, the BES would need to be fed first in the sequence since generated current in BES may vary, while the current and thereby TAN removal in HRES is tunable. In addition, feeding the BES first in the sequence is needed for the neutral pH required for biological activity at the bio-anode [6].

This work investigates for the first time a sequentially fed, combined ammonium recovery system consisting of a BES and a HRES with a shared cathode to elucidate whether this combination can save energy and if HRES can stabilize overall TAN removal efficiency and improve TAN effluent quality for unstable bio-anodes. Furthermore, the effect of feed rate, concentration and TAN loading on the performance of this combined system is investigated.

2. Materials and methods

2.1. Experimental design

The sequential BES-HRES system was constructed as a combination of the MEC previously described by Rodriguez Arredondo [34] and the HRES described in [16]. The system used here included 6 compartments in the following order: BES anode (BA), BES concentrate (BC), cathode (C), HRES concentrate (EC), HRES feed (EF) and HRES gas anode (EA) (Fig. 1). Two separate (hollow fibre) liquid/liquid membrane contactors ((HF)-LLMC) units for TAN recovery were integrated into the concentrate loops of BES and HRES, respectively.

All compartments were $14 \times 14 \text{ cm}^2$ in size, while $10 \times 10 \text{ cm}^2$ were left open as active area. The influent was continuously supplied, first through the BES anode, and the BES anode effluent fed to the HRES feed compartment to create a sequential (bio-) electro dialysis system, with the overall system effluent leaving the HRES feed compartment. The HRES gas anode continuously received H_2 from the cathode with 0.3 mL/min N_2 carrier gas as feed, which consisted mostly of H_2 (>80 %) and resulted in excess supply of H_2 during all experiments. BES concentrate, cathode, HRES concentrate, as well as BES acid and HRES acid were operated in batch. All compartments, apart from the HRES gas anode, were hydraulically recirculated at 100 mL/min using peristaltic pumps (Masterflex®, Metrohm, Belgium).

Total compartment volumes (including compartment, tubing and recirculation vessels) were each approximately 120 mL for BES anode, cathode and HRES feed, 300 mL for BES concentrate and HRES concentrate, and each 1.35 L for BES acid and HRES acid.

TAN transported from BES anode to BES concentrate and from HRES feed to HRES concentrate was recirculated through two separate, tubular (HF)-LLMC units. These units consisted of a lumen side, where the removed TAN from either BES concentrate or HRES concentrate compartment was recirculated, and a shell side, where the respective BES or HRES acid was recirculated. Thereby, gaseous NH_3 diffuses from the concentrate through the hydrophobic membrane (polypropylene membrane fiber, pore size: 200 nm , type: Accurel PP V8/HF, CUT Membrane Technology GmbH, Düsseldorf, Germany) into the acid ($1 \text{ M H}_2\text{SO}_4$). This results in the formation of an ammonium sulfate solution on the shell side of the LLMC module.

The LLMC fiber membrane had a total shell side (outer) membrane surface area of 374 cm^2 . Both BES and HRES acid were heated (to approximately $30 \text{ }^\circ\text{C}$) to equilibrate the water vapour gradient across the membrane and prevent water condensation in the acid. 1 L of each acid batch was replaced with fresh $1 \text{ M H}_2\text{SO}_4$ when the pH exceeded a pH of 1 (75 % of theoretical absorption capacity) to ensure sufficient protonation of recovered NH_3 .

The BES anode and HRES gas anode compartments consisted of titanium blocks with $10 \times 10 \times 0.4 \text{ cm}^3$ platinumized flow fields (50 gPt m^{-2} , as described in [18]) as current collectors. Both titanium blocks were

Table 1

Experimental conditions applied to combined system.

Bio-anode current	feed rate [L/d]	TAN loading [$\text{g}_\text{N}/\text{d}$]	duration [d]	medium dilution	Load ratio (HRES)
Stable	0.2	0.2	14	5 x	1.3 ± 0.2
Feed rate increase led to unstable bio-anode					
Unstable	0.2	0.2	5	5 x	1 ± 0.06
			5		2.2 ± 0.2
			5		0.7 ± 0.04
Bio-anode unstable – rebuild with fresh BES anode and BES CEM					
Stable	0.5	0.5	6	5 x	1.2 ± 0.3
	0.1		2	0 x	$7.2 \pm 4^*$
	0.5	2.5	5		1.1 ± 0.5

* low TAN concentrations and highly variable TAN effluent concentrations leaving the BES led to high variability of load ratio in HRES, see calculations.

heated with electrical pads to reach an anolyte temperature of $30 \pm 1 \text{ }^\circ\text{C}$. In addition, a $10 \times 10 \text{ cm}^2$ graphite felt of approximately 5 mm thickness (SIGRATHERM® GFA5, SGL Carbon, Germany) served as flow-through electrode material for the BES anode, separated from the membrane with spacer material (thickness 1 mm , 64 % open; PETEX 07-4000/64, Sefar BV, The Netherlands). A membrane electrode assembly (MEA) served as electrode for the HRES gas anode (Nafion™ 117 membrane on HRES feed side, platinumized carbon with 5 gPt m^{-2} on HRES gas anode side, custom 3-layer MEA, CTM-MEA, FuelCellsEtc, USA). The cathode consisted of an approximately 70 % open ruthenium-iridium coated $10 \times 10 \text{ cm}^2$ titanium mesh of 1 mm thickness and the cathode compartment was filled with spacer meshes to stabilize the membrane positions and improve mass transfer.

Selective ion transport was enabled by separating compartments either with cation exchange membranes (Ralex® CMHPP, MEGA a.s., Czech Republic) between BES anode and BES concentrate as well as HRES feed and HRES concentrate, or with anion exchange membranes (Ralex® AMHPP, MEGA a.s., Czech Republic) between BES concentrate and cathode as well as HRES concentrate and cathode compartments. Silicon gaskets ($14 \times 14 \text{ cm}^2$) with a centered opening ($10 \times 10 \text{ cm}^2$) were used on either side of each ion exchange membranes to create a watertight seal of the compartments.

All potentials in this work are reported versus 3 M Ag/AgCl , KCl-type reference electrodes ($+205 \text{ mV}$ vs NHE, Prosense QiS, Oosterhout, The Netherlands), which were placed in the influents of the BES anode, cathode and HRES feed compartments.

The BES potential and HRES current were controlled using a potentiostat (Ivium-N-stat, Ivium Technologies, the Netherlands). The BES was controlled at a constant anode potential of -0.2 V , whereas the HRES was controlled at constant current to achieve a target load ratio (L_N , see experimental strategy). Both BES and HRES were connected to the potentiostat with separate channels in separate modules of the potentiostat and the HRES operated in “floating mode” to prevent leak currents from one system to the other and thereby make operation of both systems in different operational modes possible. The pH and temperature were measured in the bio-anode recirculation using pH electrodes (Orbisint CPS11D, Endress+Hauser B.V., Naarden, The Netherlands) connected to a transmitter (Liquisys CPM253, Endress+Hauser B.V., Naarden, The Netherlands). Polyethylene (PE) tubing was used for the gas and liquid transport (DN04/06, Em-Technik, Germany) in the entire experimental setup.

2.2. Media

Synthetic urine was based on a modified recipe from [34] and contained $4.181 \text{ g/L K}_2\text{HPO}_4$, $1.207 \text{ g/L Na}_2\text{SO}_4$, $4.066 \text{ g/L MgCl}_2 \bullet 6 \text{ H}_2\text{O}$, $0.441 \text{ g/L CaCl}_2 \bullet 2 \text{ H}_2\text{O}$, 0.298 g/L KCl , 3.360 g/L NaOH , $3.136 \text{ g/L NH}_4\text{OH}$, $22.136 \text{ g/L NH}_4\text{HCO}_3$ and $5.396 \text{ g/L NH}_4\text{CH}_3\text{COOH}$. After most salts were dissolved and precipitates removed by filtering, 1 mL L^{-1} Wolfe’s trace mineral solution and 1 mL L^{-1} Wolfe’s vitamin solution

were added as micronutrient source [41]. However, 20 mL L⁻¹ of trace element and vitamin solution each were added for the last experiment shown in Table 1 (0.5 L/d undiluted medium) in order to prevent possible limitations from micronutrient availability.

2.3. Inoculum

The mixed inoculum consisted of equal volumes of biomass samples from an anaerobic digester treating black water [5], bio-electrochemical systems fed with hydrolyzed human urine and artificial urine, containing acetate as carbon and energy source [34], syntrophic propionate oxidizer cultures [24] as well as activated sludge from a wastewater treatment plant in Bath, the Netherlands.

2.4. Experimental strategy

The experimental design displayed in Table 1 was segmented into three categories: 1) stable bio-anode at low loading: After inoculation and start-up phase, the bio-anode current stabilized at 1.9 ± 0.06 A/m² for an applied relatively low feed rate of 0.2 L/d or 0.2 g_N/d TAN loading with 5x diluted synthetic urine, while a load ratio of 1.3 was applied to the HRES. After a period of 14 days, the loading was increased stepwise up to 0.6 L/d, yet the bio-anode current did not increase proportionately with increased loading, but instead declined. Returning to the original loading of 0.2 L/d still resulted in a steadily declining bio-anode current and therefore indicated an “unstable bio-anode”. 2) Unstable bio-anode with HRES compensating for high TAN removal efficiency at varying load ratios (L_N): After the bio-anode became unstable, a steadily declining current was observed that was also lower than under the same, previous conditions. The HRES L_N needed to be adapted constantly to keep the HRES L_N constant at the target value. The L_N was kept constant for 7 days each at values of 0.7, 1 and 2.2 to investigate whether compensating the lacking TAN removal from the BES with the HRES could be achieved and at which energy input.

3) Effect of feed rate, TAN loading and TAN concentration on combined system: The BES part of the system was rebuilt by replacing the CEM and anode electrode of the BES, as well as regrowing the bio-anode. The feed rate was then slowly increased from 0.1 to 0.5 L/d of 5x diluted synthetic urine until the BES showed stable and efficient current generation. Then, the influent was replaced from 5x diluted to undiluted synthetic urine to investigate the effect of feed concentration at same COD and TAN loading on the combined system performance. Finally, the feed rate was increased from 0.1 L/d to 0.5 L/d to investigate the effect of feed rate and concentration at 5x higher loading. To improve the stability of the bio-anode performance, the micronutrient concentration was increased 20x for these experiments at higher TAN and COD loading. Averages and standard deviations were calculated from different samples taken once per day under the same experimental condition and after more than 1 HRT of the BES anode.

2.5. Sampling and analysis

Sampling was carried out daily for influent, BES anode, HRES feed compartment, BES acid and HRES acid, while BES concentrate, cathode and HRES concentrate were sampled infrequently to keep track of pH and conductivity and daily to determine cation transport numbers and main ion concentrations. COD and TAN were quantified using Hach Lange cuvette tests (LCK 304 for TAN and LCK 1414 for COD, Hach Lange, United Kingdom). Electrical current was recorded from the potentiostat by IviumSoft software (Ivium Technologies, the Netherlands) and exported to Excel for data processing. Na⁺ and K⁺ concentrations were analysed using ion chromatography Metrohm Compact IC Flex 930 including a Metrosep C 4-13150/4.0 column with quantification by a conductivity detector (Metrohm Nederland BV, Schiedam, The Netherlands). The cathode and HRES gas anode effluent gas composition was analysed infrequently for H₂, O₂, N₂, CH₄, CO, CO₂

and H₂S concentrations using a dual channel Varian CP4900 micro gas chromatograph (Varian, Middelburg, the Netherlands).

2.6. Calculations

The TAN loading (Q_{TAN} in g_N/d) can be calculated as

$$Q_{TAN} = [TAN] * Q \quad (1)$$

With Q being the feed rate (L/d) and [TAN] being the TAN concentration in the feed (in g_N/L).

The recoverable TAN in (bio-)electrochemical ammonium recovery systems is dependent on the electrical current generated from converting COD from the fed wastewater. In theory, 1 mol of electrons (e⁻) can transport 1 mol of NH₄⁺. The ratio of current over ammonium loading is defined in the load ratio concept [35]:

$$L_N = \frac{i * M_{TAN}}{Q_{TAN} * z_{NH_4^+} * F} \quad (2)$$

Where i is the electrical current generated by the (bio-) anode in ampere (A), M_{TAN} the molar mass of TAN (14 g_N/mol_{TAN}), Q_{TAN} the TAN loading into the receiving compartment (BES anode or HRES feed) in g_{TAN}/d, z_{NH₄⁺} the valency of NH₄⁺ being 1, and F the Faraday number of 96,485C/mol electrons.

The L_N in BES was determined by measuring the average current generated in the bio-anode in the time during the last 1 HRT and dividing it by the TAN loading in that time period. The L_N in HRES was adjusted on a daily basis by measuring the TAN concentration in the HRES feed, which is the BES anode (assuming steady-state between influent and BES anode) and adjusting the current to reflect the desired L_N according to that TAN concentration.

The overall L_N was calculated as sum of the currents applied in BES and HRES over the TAN loaded into the combined system, which is the BES influent TAN loading:

$$L_N = \frac{(i_{BES} + i_{HRES}) * M_{TAN}}{Q_{TAN} * z_{NH_4^+} * F} \quad (3)$$

The transport number of a certain cation species across a CEM, for example NH₄⁺ from TAN, was calculated as ratio of respective cation charge that was removed over electrical charge applied as current:

$$\text{transport number} = \frac{([cation]_{\text{influent}} - [cation]_{\text{effluent}}) * Q * z_{\text{cation}} * F}{i * M_{\text{cation}}} \quad (4)$$

[cation]_{influent} is the concentration of the respective cation in the influent solution going into the BES or HRES (meaning influent or BES anode, respectively, in g_{cation}/L), [cation]_{effluent} is the concentration in the effluent of either the BES anode (for the BES) or HRES feed compartment (for the HRES, in g_{cation}/L) and z_{cation} is the valency of the respective cation. Accordingly, the transport efficiency is the multiplication of the transport number with 100 %.

The TAN removal efficiency (RE_{TAN}) was calculated from the difference of the TAN concentration present in the compartment effluent and the TAN concentration from the compartment's originating feed, assuming steady-state between TAN fed and TAN removed:

$$RE_{TAN} = \frac{[TAN]_{\text{influent}} - [TAN]_{\text{effluent}}}{[TAN]_{\text{influent}}} * 100\% \quad (5)$$

The TAN removal rate (RR_{TAN} in g_N/m²/d) was calculated as TAN removed and normalized by the total CEM area used to do so, which meant one membrane (A = 100 cm²) for BES and HRES separately and both membranes for the overall system (A = 200 cm²):

$$RR_{TAN} = \frac{([TAN]_{\text{feed}} - [TAN]_{\text{effluent}}) * Q}{A_{\text{CEM}}} \quad (6)$$

For the overall TAN removal rate, the difference between feed and HRES feed was used.

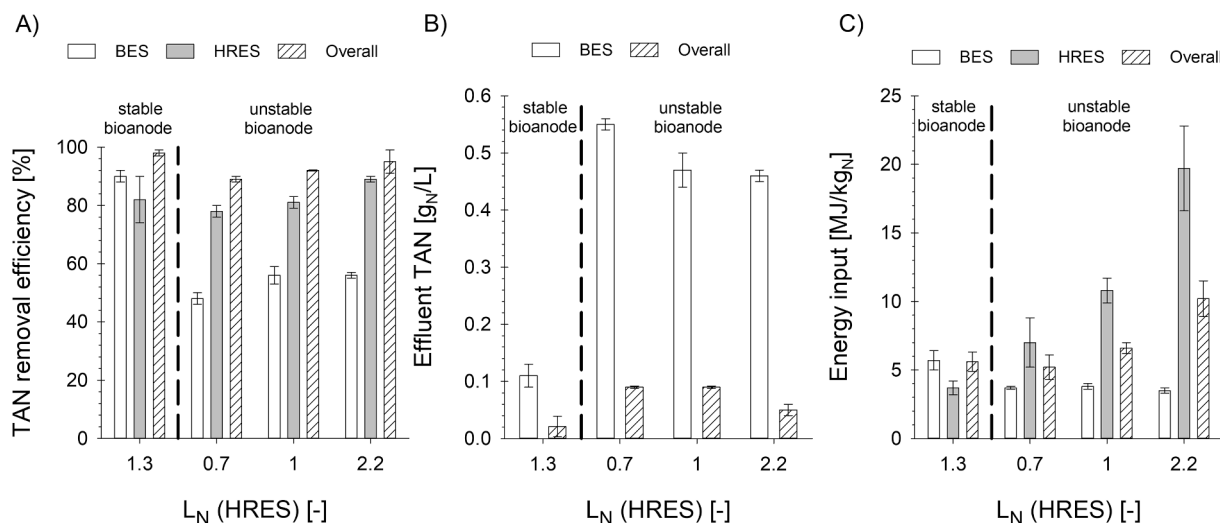


Fig. 2. Applying different load ratios in the electrochemical system at low feed rate of 0.2 L/d for stable and unstable bio-anodes with 5x diluted synthetic urine. Electrochemical system (HRES) can compensate N removal if bio-electrochemical system (BES) current becomes unstable. A) When the BES substrate conversion efficiency decreases due to biological instability, the HRES can still remove most TAN. B) Low effluent TAN concentrations (20–120 mg $_N/L$) can be achieved at low feed rates. A stable and efficient TAN removal in BES leads to the lowest effluent TAN concentration, while for an unstable BES, higher L_N applied in the HRES lead to lower effluent concentrations. C) Despite increasing L_N for the HRES, energy inputs for the overall system stay similar since part of the TAN is removed in BES at similar L_N .

The specific required energy input (in MJ/kg $_N$) was calculated as electrical energy input of the potentiostat to generate the cell potentials driving the electric currents in BES and HRES each:

$$\text{energy input} = \frac{i^*E_{\text{cell}}*t}{RR_{\text{TAN}}*A_{\text{CEM}}} \quad (7)$$

With E_{cell} being the cell voltage (in V) of the BES or HRES, and t being the amount of second per day (86400 s/d).

The overall energy input (in MJ/kg $_N$) was calculated as weighted average of the sum of energy invested (in MJ) respectively in BES and HRES over the sum of the TAN removed in each system (in kg $_N$):

$$\text{overall energy input} = \frac{(i_{\text{BES}}*E_{\text{cell,BES}} + i_{\text{HRES}}*E_{\text{cell,HRES}})*t}{(RR_{\text{TAN,BES}} + RR_{\text{TAN,HRES}})*A_{\text{CEM}}} \quad (8)$$

With A_{CEM} being 100 cm 2 .

3. Results and discussion

3.1. Electrochemical system can partially compensate for unstable anode to achieve high TAN removal

As a first test of the performance of this combined (bio-)electrodiolysis system, we investigated whether the HRES could be used to achieve high overall TAN removal when the BES generated less current (and lower TAN removal) than theoretically possible. We investigated this combined system for 5x diluted synthetic urine at a low loading rate of 0.2 L/d to enable the bio-anode to remove most substrate and thereby remove most TAN. In order to remove the remaining TAN, the current applied in the HRES was adjusted to investigate the effect of L_N on TAN removal and required specific energy input. A $L_N < 1$ was used to reflect less electrical charge applied than charge of TAN loaded into the HRES. Accordingly, applying the same electrical charge as charge of TAN loaded ($L_N = 1$), applying an optimum electrical charge per TAN loaded (for energy input and TAN removal efficiency, $L_N \approx 1.3$ [35]), and applying an excess of electrical charge per TAN loaded ($L_N \gg 1.3$) were investigated. Furthermore, we investigated the TAN removal efficiency and energy input for stable BES operation at $L_N = 1.2$, as well as unstable BES operation (below-optimum L_N in BES) using HRES TAN removal compensation at different L_N .

3.2. Stable bio-anode can remove TAN at high efficiency

At a low feed rate of 0.2 L/d and a TAN loading of 0.2 g $_N/d$ of 5x diluted synthetic urine (L_N of 1.2 ± 0.1), the BES operated indicated by the small standard deviation in current density (1.9 ± 0.1 A/m 2). The L_N of 1.2 in the BES is close to the theoretical optimum of 1.3 (based on charge of COD concentration over charge of TAN concentration in feed, [10]). The BES removed most of the TAN (90 ± 2 %) at 5.7 ± 0.7 MJ/kg $_N$ from 1 g $_N/L$ feed down to BES effluent concentrations of 0.08–0.15 g $_N/L$ (Fig. 2), which shows that the bio-anode operated efficiently.

Under this stable bio-anode condition in the BES, an applied L_N of 1.3 ± 0.2 in the HRES removed most of remaining TAN (80 %) at 3.7 ± 0.5 MJ/kg $_N$ down to effluent concentrations of 0.021 ± 0.018 g $_N/L$. Overall, the system removed 98 ± 1 % of with 10 g $_N/m^2_{\text{CEM}}/d$ (for the combined system) at 5.6 ± 0.7 MJ/kg $_N$. Therefore, at low loading and for a stable and efficient bio-anode, the overall combined system effluent TAN concentration was close to the European Urban Water Framework Directive 91/271/EEC for total N (10–15 mg $_N/L$, 70–80 % minimum removal efficiency [8]).

Thereafter, the reactor feed rate was slowly increased from 0.2 up to 0.6 L/d, but the substrate conversion efficiency of the bio-anode deteriorated progressively; the increasing feed rate led to a maximum current density of 4 A/m 2 and decreased thereafter continuously, even when reverting back to 0.2 L/d. For this unstable bio-anode, the L_N declined from 1.2 ± 0.1 to 0.4–0.5.

3.3. Increasing L_N in HRES during unstable BES operation improves TAN removal at the expense of additional energy input

In the following experiments, the bio-anode current continuously decreased despite stable feed rates, meaning less current was applied in the BES for the same TAN loading. Under these circumstances, the HRES applied current was increased to compensate the low current densities generated in the BES to remove additional TAN. The chosen applied current in HRES was modulated to either result in high overall TAN removal efficiency at higher applied L_N ($\gg 1.3$), or to result in low overall required energy input at lower applied L_N ($\ll 1.3$). The unstable bio-anode (L_N 0.4–0.5) only removed 48–56 % of TAN (Fig. 2 A) at 3.5–3.8 MJ/kg $_N$ (Fig. 2 C) down to BES effluent concentrations of 0.46–0.55 g $_N/L$ (Fig. 2 B).

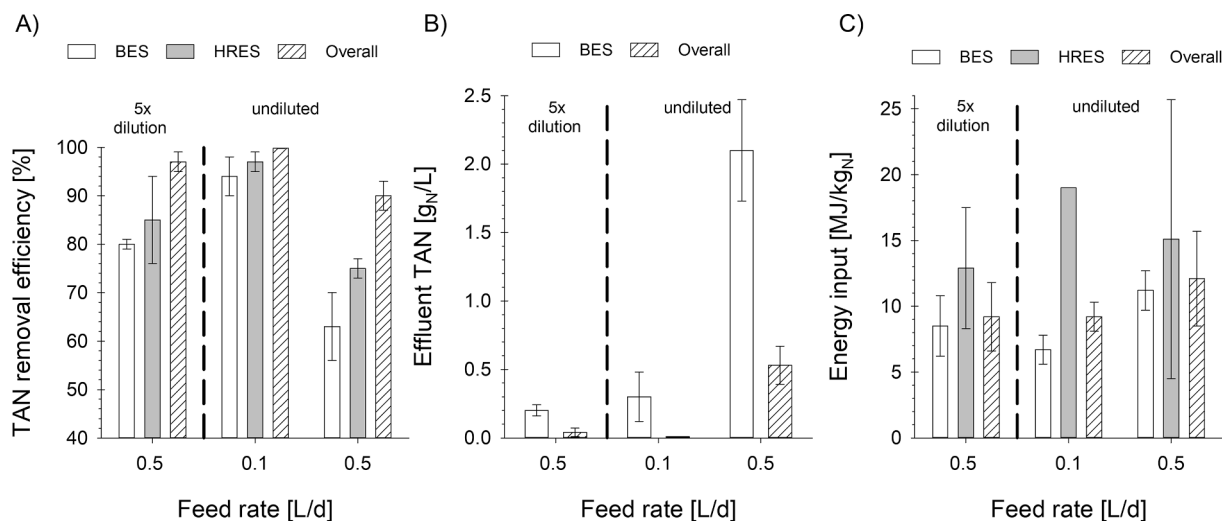


Fig. 3. Applying different dilutions and feed rates on combined BES/HRES system to compare same TAN loading or feed rates. A) TAN removal efficiencies increased for more concentrated feed at same loading, while it decrease at same feed rate and higher loading. B) Very low effluent TAN concentrations (10–40 mg_N/L) can be achieved at low TAN loading rates. C) The required energy input for the combined system increase only with less dilution and higher feed rate.

When focusing on the HRES, increasing the L_N in the HRES from 0.7 to 1 increased the HRES required energy input by 88 % (Fig. 2 C), yet only an additional 4 % of the TAN loaded into the HRES was removed (Fig. 2 A). Applying a L_N of 0.7 ± 0.04 to this BES effluent in the HRES, which is only 70 % of the electrical charge supplied for the charge of TAN loaded into the reactor, 78 ± 2 % TAN (Fig. 2 A) were removed at 7 ± 1.8 MJ/kg_N (Fig. 2 C) down to an overall effluent concentration of 120 ± 10 mg_N/L (Fig. 2 B). Removing 78 % of TAN while applying 70 % of required charge ($L_N = 0.7$) means a transport efficiency of 111 %, which is likely a result of the high contribution of TAN diffusion from analyte to concentrate at an applied L_N below 1.

When applying an L_N of 1 ± 0.06 in the HRES to supply exactly enough current to remove the loaded TAN from the unstable BES, 81 ± 2 % of TAN was removed (Fig. 2 A) at 10.8 ± 0.9 MJ/kg_N (Fig. 2 C) down to 90 ± 2 mg_N/L overall effluent concentration (Fig. 2 B) in the HRES. Therefore, applying 43 % more current ($L_N 0.7 \rightarrow 1$) removes only 3 % more TAN (78 % vs 81 %), but increases the required power input by 54 % from 7 ± 1.8 MJ/kg_N to 10.8 ± 0.9 MJ/kg_N in the HRES. The effluent concentrations decreased by 25 % from 120 mg_N/L to 90 mg_N/L. Therefore, increasing the L_N from 0.7 to 1 increased the energy input relatively more than the TAN removal efficiency. This is contrary to previous findings, where below $L_N 1$ the energy invested increased proportionately with the TAN removal efficiency [32,33,35].

Increasing the L_N in the HRES further from 1 to 2.2 ± 0.2 resulted in a strong increase in required energy input, while the TAN removal efficiency increased slightly and the TAN effluent concentration decreased further. At $L_N 2.2$, 89 ± 1 % of TAN was removed at 19.7 ± 3.1 MJ/kg_N down to overall effluent TAN concentration of 50 ± 10 mg_N/L. This increased the required energy input by 83 % (from 10.8 ± 0.9 MJ/kg_N to 19.7 ± 3.1 MJ/kg_N, Fig. 2 C) at 8 % additional TAN removed (from 81 ± 2 % to 89 ± 1 %, Fig. 2 A). The effluent concentrations decreased by 44 % from 90 mg_N/L to 50 mg_N/L (Fig. 2 B).

In conclusion, applying a higher L_N to increase removal of remaining TAN from the BES effluent costs disproportionately more energy input in the HRES.

3.4. Overall performance of increasing L_N in HRES to compensate for unstable BES

Increasing the L_N of the HRES increased the overall specific energy input (weighted average of BES and HRES) less than the energy input for the HRES alone. The overall energy input increased from 5.2 ± 0.9 MJ/

kg_N at $L_N 0.7$, to 6.6 ± 0.4 MJ/kg_N at $L_N 1$, and to 10.2 ± 1.3 MJ/kg_N at $L_N 2.2$. Meanwhile, the overall TAN removal efficiency increased from 89 ± 1 % at $L_N 0.7$, to 92 ± 0.2 % at $L_N 1$, and at $L_N 2.2$ to 95 ± 4 %. This shows that in this combined system, increasing the applied L_N in the HRES from 0.7 to 1 comes at a 17 % higher overall energy input, while 3 % more TAN is removed overall. Increasing the L_N from 1 to 2.2 increases the overall energy input by 56 %, while 3 % more TAN is removed overall. This confirms the findings of [35] that applying a L_N higher than 1 increases the energy input, but realizes a higher removal efficiency. These high overall TAN removal efficiencies at low overall energy inputs confirm the potential of the combined system to achieve high TAN removal at low energy input.

3.5. TAN removal efficiency is dependent on feed concentration and loading, while energy input is independent from both at constant L_N

In the following experiments, we investigated the effect of feed concentration, feed loading, and feed rate on the TAN removal efficiency and energy input at an applied L_N of 1.2 in the HRES. First, the feed concentration was increased from 5x dilution to no dilution at same TAN loading of 0.5 g_N/d by changing the feed rate from 0.5 L/d to 0.1 L/d. Then, the feed loading was increased to 2.5 g_N/d TAN loading with the undiluted feed by increasing the feed rate from 0.1 L/d to 0.5 L/d. In order to prevent possible limitations in the BES, as observed in the first set of experiments for higher loadings, an excess of 20x micronutrients was added to sustain stable bio-anode performance.

3.6. Effect of feed concentration at lower feed rate, but same loading

For the BES, increasing the feed concentration from 5x diluted to undiluted feed resulted in increased TAN removal efficiency at decreased energy input. The TAN removal efficiency increased by 14 % from 80 ± 1 % to 94 ± 4 %, while the required energy input decreased by 27 % from 8.5 ± 2.3 to 6.7 ± 1.1 MJ/kg_N (Fig. 3). The change in concentration did neither affect the generated current density (4 ± 0.3 to 3.5 ± 2 A/m²) and thereby L_N in the BES (0.9 ± 0.2 to 0.9 ± 0.04) nor the effluent TAN concentration (0.2 ± 0.04 to 0.3 ± 0.18 g_N/L) for the BES. The equal L_N is a result of feeding the same loading of COD and TAN to a stable and efficient bio-anode. However, the similar effluent TAN concentration and higher TAN removal efficiency might not be a result of the bio-anode performance, but rather of the higher contribution of diffusion to TAN removal at greater TAN concentration gradients

(Appendix A – Figure A.1, C).

This is also indicated by the increase in TAN transport efficiency from $93 \pm 24 \%$ to $103 \pm 8 \%$ (Appendix A – Figure A.1, A). This contribution of diffusion to the overall TAN transport is higher at lower current densities and can be expected to decrease at higher applied current densities.

For the overall system performance, the TAN removal efficiency changed significantly from $97 \pm 2 \%$ to $99.8 \pm 0.02 \%$ (p-value student t-test: 0.02). This 99.8 % removal efficiency led to the lowest overall effluent TAN concentration found throughout all experiments here with $10 \pm 0 \text{ mg}_\text{N}/\text{L}$, which would comply to the European Urban Water Framework Directive 91/271/EEC.

3.7. Effect of higher loading at higher feed rate, but same concentration

When increasing the feed rate, and thereby loading, from 0.1 to 0.5 L/d for concentrated feed, we added 20x the micronutrients to the feed to avoid bio-anode limitations (as observed for higher loadings in the previous experiments). This was necessary to be able to distinguish the effect of increased TAN loading on the combined system performance, rather than observing changes in the BES performance.

Increasing the feed rate by a factor of 5 increased the conversion of substrate to electricity in the BES by almost the same factor from 3.5 ± 2 to $18 \pm 2 \text{ A}/\text{m}^2$ (factor 5.1). However, the TAN removal efficiency in the BES decreased by 31 % from $94 \pm 4 \%$ to 63 ± 7 , while the BES effluent TAN concentration increased from $0.2 \pm 0.04 \text{ g}_\text{N}/\text{L}$ to $2.1 \pm 0.4 \text{ g}_\text{N}/\text{L}$. The lower removal of TAN and therefore higher TAN effluent concentration can be explained by the higher contribution of TAN transport by migration rather than diffusion at higher feed rates, which is also indicated by the decrease in net TAN transport efficiency for the higher feed rate (from $103 \pm 8 \%$ to $73 \pm 6 \%$, see Appendix A – Figure A.1, A). This means that cations other than NH_4^+ are transported by migration, which lowers the TAN removal efficiency and can be regarded as energy input that is not invested in TAN removal. Therefore, the energy input also increases at the higher feed rate from $6.7 \pm 1.1 \text{ MJ}/\text{kg}_\text{N}$ to $11.2 \pm 1.5 \text{ MJ}/\text{kg}_\text{N}$ (67 %) (Fig. 3 C).

For the overall system, the TAN removal efficiency decreases from $99.8 \pm 0.02 \%$ to $90 \pm 3 \%$, while the TAN effluent concentration increases from 10 ± 0 to $530 \pm 140 \text{ g}_\text{N}/\text{L}$ at similar energy input (9.2 ± 1.1 vs $12.1 \pm 3.6 \text{ MJ}/\text{kg}_\text{N}$). The decrease in TAN removal efficiency and increase in TAN effluent concentration are caused by the lower TAN removal efficiency of the BES leading to higher TAN loading and thereby more TAN needing to be removed in the HRES.

3.8. Effect of higher loading and higher concentration, but same feed rate

We also investigated the effect of higher loading rates (of TAN and COD) by supplying the same feed rate of 0.5 L/d undiluted synthetic urine instead of 5x diluted. This was done to investigate the effect of higher loadings on the combined system. This decreased the TAN removal efficiency despite similar applied L_N . The TAN removal efficiency in the BES decreased from $80 \pm 1 \%$ at $L_\text{N} 0.9 \pm 0.2$ to $63 \pm 7 \%$ at $L_\text{N} 0.9 \pm 0.1$ (Fig. 3) at an increase of TAN removal rate from 46 to $168 \text{ g}_\text{N}/\text{m}^2_\text{CEM}/\text{d}$ (see Appendix A – Table A.1). Thereby, the required energy input for BES increased by 29 % from 8.5 ± 2.3 to $11.2 \pm 1.5 \text{ MJ}/\text{kg}_\text{N}$ as combination of higher generated currents (increase from 4 ± 0.3 to $18 \pm 2 \text{ A}/\text{m}^2$) and applied cell voltages, as well as lower TAN removal efficiency. The TAN effluent concentration leaving the BES increased accordingly from 0.2 ± 0.04 to $2.1 \pm 0.4 \text{ g}_\text{N}/\text{L}$.

The overall TAN removal efficiency decreased with increasing loading from $97 \pm 2 \%$ to $90 \pm 3 \%$ (Fig. 3 A) and the overall TAN removal rates increased from 28 ± 5 to $121 \pm 4 \text{ g}_\text{N}/\text{m}^2_\text{CEM}/\text{d}$ (see Appendix A – Table A.1) at similar L_N applied in the HRES (1.2 ± 0.3 to 1.1 ± 0.5) leading to an overall effluent TAN concentration of 0.53 ± 0.14 .

Table 2
Performance parameters of experiments in this work compared to other publications.

	current density [A/m^2]	load ratio (L_N)	TAN loading [$\text{g}_\text{N}/\text{d}$]	feed TAN concentration [$\text{g}_\text{N}/\text{L}$]	TAN concentration	TAN removal efficiency [%]	TAN removal rate [$\text{m}^2_\text{CEM}/\text{d}$]	specific energy input [$\text{MJ}/\text{kg}_\text{N}$]	effluent TAN [$\text{g}_\text{N}/\text{L}$]
[14] BES	3	1.4	0.2	1.2		76	29	16 *	0.3 *
	5	0.4	1			27	38	19 *	0.8 *
[34] BES	11	0.6	2.3	2.5		61	118	6.8	1.5 *
[12] BES	27	0.8	2.8 *	5.1		51	226	22	2.7
[19] BES	29	0.4	8.7 *	5.9		60	522 *	8.6	2.4 *
[21] ES	30	0.8	2.9 *	8.0		78	310	29	1.8 *
[17] HRES	20	1.3	9.2	4.0		61 *	141	15	1.6 *
this work	0.8	0.5	0.2	1.1		56	12	3.8	0.5
condition a	overall $0.8 + 0.7$	0.9				92	10	6.6	0.1
condition b	BES 4	0.9		5.5		94	44	6.7	0.3
condition c	overall $4 + 1$	1.2				99.8	23	9.2	0.01
	BES 18	0.9	2.7			63	168	11	2.1
	overall $18 + 8$	1.2				90	121	12	0.5

*"Overall" TAN removal rate of this work is normalized by the sum of both CEMs used here. * calculated from provided data in respective publication. Condition a: unstable BES, HRES $L_\text{N} = 1$; condition b, c: stable BES.

3.9. Combined (bio-)electrodialysis system can remove TAN at high efficiency at low energy input

To provide broader context for the performance of this new combined system, a comparison with published literature on other (B)ES fed continuously with synthetic urine is provided in Table 2. When the BES in this work is only converting a fraction of the supplied COD to electricity (Table 2, condition a) or is experiencing TAN loadings comparable to literature (Table 2, condition c), TAN removal efficiencies in the BES are comparable to literature (56–63 % vs 51–76 %).

Under these conditions, the HRES can compensate the lacking TAN removal in the BES up to 90–92 % overall TAN removal efficiency, reaching spectacular lower effluent TAN concentrations compared to separate systems (0.1–0.5 g_N/L vs 1.5–2.7 g_N/L). The TAN removal rate for the BES (168 g_N/m²/d) is comparable to literature with similar reactor configuration (118–226 g_N/m²/d), while the overall rate is lower (121 g_N/m²/d) because of the normalization against both CEM used in the HRES and BES each.

While individually some reported performance parameters (i.e., current density, rates, specific energy input) in literature exceeded the results obtained in this work, the unique combination of an overall low specific energy input and high removal efficiency obtained in this work are unmatched.

Furthermore, when the BES is converting most substrate at low feed rate (Table 2, condition b), most TAN is removed in the BES (94 %) and applying a L_N of 1.0 in the HRES removes almost all remaining TAN down to 0.01 g_N/L with 99.8 % overall efficiency. This overall TAN removal efficiency and effluent quality are exceptionally high for a continuously fed (B)ES.

4. Conclusion

Combining both BES and HRES in one system with a shared cathode permits use of the hydrogen gas produced in the BES as hydrogen feed for the HRES and to compensate for loss during hydrogen recycling. This novel design of the combined BES-ES systems lowers the spatial footprint when compared to two separate sequential systems. The very low effluent concentrations reached here of 10 mg_N/L (up to 99.8 % TAN removal efficiency), as well as the low overall energy input of 6.6 – 12.1 MJ/kg_N indicate a better performance of the combined system than in published research on comparative wastewaters in (B)ES known to the authors.

This combined system solves the issue of bio-anode stability for ammonium recovery in BES, lowers the energy input when compared to purely electrochemical ammonium recovery systems and opens new possibilities for TAN removal applications.

Therefore, following research should investigate whether the HRES could still compensate for unstable or inefficient TAN removal in BES for non-synthetic wastewaters. The conducted experiments here indicate that this combined system could be a viable technology to efficiently remove TAN from wastewaters.

Declaration of Competing Interest

The authors declare that they have no known competing financial interests or personal relationships that could have appeared to influence the work reported in this paper.

Data availability

The data underlying this study will be made openly available in 4TU. ResearchData at doi: 10.4121/14822871

Acknowledgements

This work was performed in the cooperation framework of Wetsus,

European Centre of Excellence for Sustainable Water Technology (www.wetsus.eu). Wetsus is co-funded by the Dutch Ministry of Economic Affairs and Ministry of Infrastructure and Environment, the European Union Regional Development Fund, the province of Fryslân, and the Northern Netherlands Provinces. This research has received funding from the European Union's Horizon 2020 research and innovation programme under the Marie Skłodowska-Curie grant agreement No 665874. The authors like to thank the participants of the research theme "Resource Recovery" for the fruitful discussions and their financial support.

Appendix A. Supplementary data

Supplementary data to this article can be found online at <https://doi.org/10.1016/j.cej.2022.140196>.

References

- [1] V. Amstutz, A. Katsounis, A. Kapalka, C. Comninellis, K.M. Udert, Effects of carbonate on the electrolytic removal of ammonia and urea from urine with thermally prepared IrO₂ electrodes, *J. Appl. Electrochem.* 42 (2012) 787–795, <https://doi.org/10.1007/s10800-012-0444-y>.
- [2] B.M. Campbell, D.J. Beare, E.M. Bennett, J.M. Hall-Spencer, J.S.I. Ingram, F. Jaramillo, R. Ortiz, N. Ramankutty, J.A. Sayer, D. Shindell, Agriculture production as a major driver of the earth system exceeding planetary boundaries, *Ecol. Soc.* 22 (2017), <https://doi.org/10.5751/ES-09595-220408>.
- [3] J.G. Chen, R.M. Crooks, L.C. Seefeldt, K.L. Bren, R. Morris Bullock, M. Y. Darenbourg, P.L. Holland, B. Hoffman, M.J. Janik, A.K. Jones, M.G. Kanatzidis, P. King, K.M. Lancaster, S.V. Lyman, P. Pfomm, W.F. Schneider, R.R. Schrock, Beyond fossil fuel-driven nitrogen transformations, *Science* 80- (2018) 360, <https://doi.org/10.1126/science.aar6611>.
- [4] M.E.R. Christiaens, S. Gildemyn, S. Matassa, T. Ysebaert, J. De Vrieze, K. Rabaey, Electrochemical ammonia recovery from source-separated urine for microbial protein production, *Environ. Sci. Technol.* 51 (2017) 13143–13150, <https://doi.org/10.1021/acs.est.7b02819>.
- [5] J.R. Cunha, C. Schott, R.D. van der Weijden, L.H. Leal, G. Zeeman, C. Buisman, Calcium addition to increase the production of phosphate granules in anaerobic treatment of black water, *Water Res.* 130 (2018) 333–342, <https://doi.org/10.1016/j.watres.2017.12.012>.
- [6] A.C.L. De Lichtervelde, A. Ter Heijne, H.V.M. Hamelers, P.M. Biesheuvel, J. E. Dykstra, Theory of ion and electron transport coupled with biochemical conversions in an electroactive biofilm, *Phys. Rev. Appl.* 12 (2019) 1, <https://doi.org/10.1103/PhysRevApplied.12.014018>.
- [7] J. Desloover, A.A. Woldeyohannis, W. Verstraete, A. Abate Woldeyohannis, W. Verstraete, N. Boon, K. Rabaey, Electrochemical resource recovery from digestate to prevent ammonia toxicity during anaerobic digestion, *Environ. Sci. Technol.* 46 (2012) 12209–12216, <https://doi.org/10.1021/es3028154>.
- [8] European Council, 1991. Urban Waste Water Treatment Directive 91/271/EEC of the European Parliament and of the Council concerning urban waste-water treatment, Official Journal of the European Parliament.
- [9] Fertilizers Europe, 2000. Best available techniques for pollution prevention and control in the European fertilizer industry: Production of NPK by the mixed acid route, 2000 Edition. Water Sci. Technol. 40.
- [10] S. Georg, C. Schott, J.R.C. Capitaio, T. Sleutels, P. Kuntke, A. Heijne, N. Buisman, Bio-electrochemical degradability of prospective wastewaters to determine their ammonium recovery potential, *Sustain. Energy Technol. Assess.* 47 (2021), 101423, <https://doi.org/10.1016/j.seta.2021.101423>.
- [11] G. Gil, I. Chang, B.H. Kim, M. Kim, J. Jang, H.S. Park, H.J. Kim, Operational parameters affecting the performance of a mediator-less microbial fuel cell, *Biosens. Bioelectron.* 18 (2002) 327–334.
- [12] S. Gildemyn, A.K. Luther, S.J. Andersen, J. Desloover, K. Rabaey, Electrochemically and bioelectrochemically induced ammonium recovery, *J. Vis. Exp.* 52405 (2015), <https://doi.org/10.3791/52405>.
- [13] H.V.M. Hamelers, A. ter Heijne, N. Stein, R.A. Rozendal, C.J.N. Buisman, Butler–Volmer–Monod model for describing bio-anode polarization curves, *Bioresour. Technol.* 102 (2011) 381–387, <https://doi.org/10.1016/j.biortech.2010.06.156>.
- [14] V. Koskue, J.M. Rinta-Kanto, S. Freguia, P. Ledezma, M. Kokko, Optimising nitrogen recovery from reject water in a 3-chamber bioelectroconcentration cell, *Sep. Purif. Technol.* 264 (2021), 118428, <https://doi.org/10.1016/j.seppur.2021.118428>.
- [15] P. Kuntke, M. Rodrigues, T. Sleutels, M. Saakes, H.V.M. Hamelers, C.J.N. Buisman, Energy-efficient ammonia recovery in an up-scaled hydrogen gas recycling electrochemical system, *ACS Sustain. Chem. Eng.* 6 (2018) 7638–7644, <https://doi.org/10.1021/acssuschemeng.8b00457>.
- [16] P. Kuntke, M. Rodríguez Arredondo, L. Widayakristi, A. ter Heijne, T.H.J.A. Sleutels, H.V.M. Hamelers, C.J.N. Buisman, Hydrogen gas recycling for energy efficient ammonia recovery in electrochemical systems, *Environ. Sci. Technol.* 51 (2017) 3110–3116, <https://doi.org/10.1021/acs.est.6b06097>.
- [17] P. Kuntke, T.H.J.A. Sleutels, M. Rodríguez Arredondo, S. Georg, S.G. Barbosa, A. ter Heijne, H.V.M. Hamelers, C.J.N. Buisman, (Bio)electrochemical ammonia

- recovery: progress and perspectives, *Appl. Microbiol. Biotechnol.* 102 (2018) 3865–3878, <https://doi.org/10.1007/s00253-018-8888-6>.
- [18] P. Kuntke, T.H.J.A. Sleutels, M. Saakes, C.J.N. Buisman, Hydrogen production and ammonium recovery from urine by a microbial electrolysis cell, *Int. J. Hydrogen Energy* 39 (2014) 4771–4778, <https://doi.org/10.1016/j.ijhydene.2013.10.089>.
- [19] P. Ledezma, J. Jermakka, J. Keller, S. Freguia, Recovering nitrogen as a solid without chemical dosing: bio-electroconcentration for recovery of nutrients from urine, *Environ. Sci. Technol. Lett.* 4 (2017) 119–124, <https://doi.org/10.1021/acs.estlett.7b00024>.
- [20] H. Liu, S. Grot, B.E. Logan, Electrochemically assisted microbial production of hydrogen from acetate, *Environ. Sci. Technol.* 39 (2005) 4317–4320, <https://doi.org/10.1021/es050244p>.
- [21] A.K. Luther, J. Desloover, D.E. Fennell, K. Rabaey, Electrochemically driven extraction and recovery of ammonia from human urine, *Water Res.* 87 (2015) 367–377, <https://doi.org/10.1016/j.watres.2015.09.041>.
- [22] M. Maurer, P. Schwegler, T.A. Larsen, Nutrients in urine: Energetic aspects of removal and recovery, *Water Sci. Technol.* 48 (2003) 37–46, <https://doi.org/10.2166/wst.2003.0011>.
- [23] S. Molenaar, T. Sleutels, J. Pereira, M. Iorio, C. Borsje, J. Zamudio, F. Fabregat-Santiago, C. Buisman, A. Ter Heijne, In situ biofilm quantification in Bioelectrochemical Systems using Optical Coherence Tomography, *ChemSusChem* 5 (2018) 644–656, <https://doi.org/10.1002/cssc.201800589>.
- [24] Mollaei, M., Ni, M.M., Sleutels, T.H.J.A., Stams, A.J.M., Plugge, C.M., 2017. Syntrophic cocultures of *Geobacter sulfurreducens* and *Syntrophobacter fumaroxidans* growing on propionate and Fe (III) or a solid electrode as electron acceptors, in: *Microbiology Centennial Symposium 2017 - Exploring Microbes for the Quality of Life*. doi: 10.18174/424506.
- [25] J.F. Ortiz-Medina, D.F. Call, Electrochemical and microbiological characterization of bioanode communities exhibiting variable levels of startup activity, *Front. Energy Res.* 7 (2019) 1–11, <https://doi.org/10.3389/fenrg.2019.00103>.
- [26] T.H. Pham, P. Aelterman, W. Verstraete, Bioanode performance in bioelectrochemical systems: recent improvements and prospects, *Trends Biotechnol.* 27 (2009) 168–178, <https://doi.org/10.1016/j.tibtech.2008.11.005>.
- [27] W. Pronk, M. Biebow, M. Boller, Treatment of source-separated urine by a combination of bipolar electro dialysis and a gas transfer membrane, *Water Sci. Technol.* 53 (2006) 139–146, <https://doi.org/10.2166/wst.2006.086>.
- [28] Rabaey, K., Plugge, C.M., van Lier, J.B., Stams, A.J.M., Jeison, D., Zulfic, Z., Minteer, S.D., Marsili, E., Zhang, X., Bretschger, O., Gorby, Y.A., Neelson, K.H., Rosenbaum, M., Angenent, L.T., Schroder, U., Harnisch, F., LaBelle, E., Bond, D.R., Lowy, D.A., Manohar, A.K., He, Z., Mansfeld, F., Logan, B.E., Hamelers, B., Sleutels, T.H.J.A., Jeremiasse, A.W., Post, J.W., Strik, D.P.B.T.B., Rozendal, R.A., Freguia, S., Dutta, P.K., Keller, J., Yuan, Z., Clauwaert, P., Aulenta, F., Majone, M., Girguis, P.R., Nielsen, M.A.E., Reimers, C.E., Kim, B.H., Chang, I.N.S., Gadd, G.M., Hawkes, F.R., Kim, J.R., Kyazze, G., Premier, G.C., Agler, M.T., Fornero, J.J., Venkataraman, A., Ieropoulos, I., Greenman, J., Melhuish, C., Horsfield, I., Rodriguez, J., Lens, P., 2010. *Bioelectrochemical Systems, Bioelectrochemical Systems From Extracellular Electron Transfer to Biotechnological Application*. IWA Publishing. doi: 10.1007/978-981-15-6872-5.
- [29] M. Reig, X. Vecino, O. Gibert, C. Valderrama, J.L. Cortina, Study of the operational parameters in the hollow fibre liquid-liquid membrane contactors process for ammonia valorisation as liquid fertiliser, *Sep. Purif. Technol.* 255 (2021), 117768, <https://doi.org/10.1016/j.seppur.2020.117768>.
- [30] J. Rockström, W. Steffen, K. Noone, Å. Persson, F.S.I. Chapin, E. Lambin, T. M. Lenton, M. Scheffer, C. Folke, H.J. Schellnhuber, B. Nykvist, C.A. de Wit, T. Hughes, S. van der Leeuw, H. Rodhe, S. Sörlin, P.K. Snyder, R. Costanza, U. Svedin, M. Falkenmark, L. Karlberg, R.W. Corell, V.J. Fabry, J. Hansen, B. Walker, D. Liverman, K. Richardson, P. Crutzen, J. Foley, Planetary boundaries: exploring the safe operating space for humanity, *Ecol. Soc.* 14 (2009) art32, <https://doi.org/10.5751/ES-03180-140232>.
- [31] M. Rodrigues, T.T. De Mattos, T. Sleutels, A. Ter Heijne, H.V.M. Hamelers, C.J. N. Buisman, P. Kuntke, Minimal bipolar membrane cell configuration for scaling up ammonium recovery, *ACS Sustain. Chem. Eng.* 8 (2020) 17359–17367, <https://doi.org/10.1021/acssuschemeng.0c05043>.
- [32] M. Rodrigues, A. Paradkar, T. Sleutels, A.T. Heijne, C.J.N. Buisman, H.V. M. Hamelers, P. Kuntke, Donnan Dialysis for scaling mitigation during electrochemical ammonium recovery from complex wastewater, *Water Res.* 201 (2021), <https://doi.org/10.1016/j.watres.2021.117260>.
- [33] M. Rodrigues, T. Sleutels, P. Kuntke, D. Hoekstra, A. ter Heijne, C.J.N. Buisman, H. V.M. Hamelers, Exploiting Donnan Dialysis to enhance ammonia recovery in an electrochemical system, *Chem. Eng. J.* 395 (2020), 125143, <https://doi.org/10.1016/j.cej.2020.125143>.
- [34] M. Rodríguez Arredondo, P. Kuntke, A. ter Heijne, C.J.N. Buisman, The concept of load ratio applied to bioelectrochemical systems for ammonia recovery, *J. Chem. Technol. Biotechnol.* 94 (2019) 2055–2061, <https://doi.org/10.1002/jctb.5992>.
- [35] M. Rodríguez Arredondo, P. Kuntke, A. ter Heijne, H.V.M. Hamelers, C.J. N. Buisman, Load ratio determines the ammonia recovery and energy input of an electrochemical system, *Water Res.* 111 (2017) 330–337, <https://doi.org/10.1016/j.watres.2016.12.051>.
- [36] Rozendal, R.A., Buisman, C.J.N., 2005. Process for producing hydrogen.pdf. WO 2005/005981 A2.
- [37] San-Martín, M.I., Leicester, D.D., Heidrich, E.S., Alonso, R.M., Mateos, R., Escapa, A., 2018. *Bioelectrochemical Systems for Energy Valorization of Waste Streams*, in: Tsvetkov, P. (Ed.), *Energy Systems and Environment*. intechopen, pp. 127–142. doi: <https://doi.org/10.5772/57353>.
- [38] W.R. Stahel, Circular economy, *Nature* 531 (2016) 435–438, <https://doi.org/10.1038/531435a>.
- [39] W. Steffen, K. Richardson, J. Rockström, S.E. Cornell, I. Fetzer, E.M. Bennett, R. Biggs, S.R. Carpenter, W. De Vries, C.A. De Wit, C. Folke, D. Gerten, J. Heinke, G. M. Mace, L.M. Persson, V. Ramanathan, B. Reyers, S. Sörlin, Planetary boundaries: Guiding human development on a changing planet, *Science* 80- (2015) 347, <https://doi.org/10.1126/science.1259855>.
- [40] H. Tian, R. Xu, J.G. Canadell, R.L. Thompson, W. Winiwarter, P. Suntharalingam, E.A. Davidson, P. Ciais, R.B. Jackson, G. Janssens-Maenhout, M.J. Prather, P. Regnier, N. Pan, S. Pan, G.P. Peters, H. Shi, F.N. Tubiello, S. Zaehle, F. Zhou, A. Arneeth, G. Battaglia, S. Berthet, L. Bopp, A.F. Bouwman, E.T. Buitenhuis, J. Chang, M.P. Chipperfield, S.R.S. Dangaal, E. Dlugokencky, J.W. Elkins, B.D. Eyre, B. Fu, B. Hall, A. Ito, F. Joos, P.B. Krummel, A. Landolfi, G.G. Laruelle, R. Lauerwald, W. Li, S. Lienert, T. Maavara, M. MacLeod, D.B. Millet, S. Olin, P. K. Patra, R.G. Prinn, P.A. Raymond, D.J. Ruiz, G.R. van der Werf, N. Vuichard, J. Wang, R.F. Weiss, K.C. Wells, C. Wilson, J. Yang, Y. Yao, A comprehensive quantification of global nitrous oxide sources and sinks, *Nature* 586 (2020) 248–256, <https://doi.org/10.1038/s41586-020-2780-0>.
- [41] E.A. Wolin, M.J. Wolin, R.S. Wolfe, Formation of methane by bacterial extracts, *J. Biol. Chem.* 238 (8) (1963) 2882–2886.
- [42] P. Zamora, T. Georgieva, A. Ter Heijne, T.H.J.A. Sleutels, A.W. Jeremiasse, M. Saakes, C.J.N. Buisman, P. Kuntke, Ammonia recovery from urine in a scaled-up Microbial Electrolysis Cell, *J. Power Sources* 356 (2017) 491–499, <https://doi.org/10.1016/j.jpowsour.2017.02.089>.
- [43] H. Zöllig, A. Remmele, C. Fritzsche, E. Morgenroth, K.M. Udert, Formation of chlorination byproducts and their emission pathways in chlorine mediated electro-oxidation of urine on active and nonactive type anodes, *Environ. Sci. Technol.* 49 (2015) 11062–11069, <https://doi.org/10.1021/acs.est.5b01675>.
- [44] S. Zou, M. Qin, Y. Moreau, Z. He, Nutrient-energy-water recovery from synthetic sidestream centrate using a microbial electrolysis cell - forward osmosis hybrid system, *J. Clean. Prod.* 154 (2017) 16–25, <https://doi.org/10.1016/j.jclepro.2017.03.199>.